Histochem Cell Biol (1999) 111:153–162

ORIGINAL PAPER

Rui P. Fernandes · Douglas A. Cotanche
Kelley Lennon-Hopkins · Fatih Erkan · A. Sue Menko
Maria A. Kukuruzinska

Differential expression of proliferative, cytoskeletal, and adhesive proteins during postnatal development of the hamster submandibular gland

Accepted: 26 October 1998

Abstract Although the submandibular gland (SMG) plays important exocrine and endocrine roles, little is known about the molecular details underlying its development. Previously, we reported that in the postnatally developing hamster SMG, GPT, the protein product of the first *N*-glycosylation gene, ALG7, was an in vivo marker for salivary cell proliferation. Here we investigated the proliferative, cytoskeletal, and adhesive changes during SMG postnatal development. The cellular localization and abundance of GPT, filamentous actin, and β1 integrin receptor were examined using confocal microscopy and immunoblotting. In neonatal glands, high GPT levels marked extensive cell proliferation throughout the tissue. The apical regions of immature salivary cells displayed intense actin staining, while most of the β1 integrin was diffusely distributed throughout the tissue. As development proceeded, discrete regions of the gland expressed attenuated levels of GPT, an increased organization of actin to the cell cortex, and β1 integrin to the basal lamina. In the adult SMG, differentiated salivary cells displayed low levels of GPT and actin. While the abundance of β1 integrin remained unchanged throughout development, in the adult, it was found exclusively in regions where cells contact the basal lamina. These data indicate that SMG development entails regionalized cell proliferation and polarization, and that these processes are temporally and spatially coordinated with the establishment of stable cell-substratum interactions.

R.P. Fernandes · K. Lennon-Hopkins · F. Erkan
M.A. Kukuruzinska (✉)
Department of Molecular and Cell Biology,
Boston University School of Dental Medicine,
700 Albany Street, Boston, MA 02118 USA
e-mail: mkukuruz@bu.edu
Tel.: (617) 638-4859, Fax: (617)414-1041

D.A. Cotanche
Department of Otolaryngology and Communication Disorders,
Children's Hospital, Boston, MA 02114 USA

A.S. Menko
Department of Pathology, Anatomy and Cell Biology,
Jefferson Medical College, Philadelphia, PA 19107 USA

Introduction

The submandibular gland (SMG) develops through the process of branching morphogenesis, involving interactions of the oral epithelium with the mesenchyme (Chaudry et al. 1985; Denny et al. 1997; Devi and Jacoby 1966). In hamster, the SMG begins to form in the last third of the embryonic period as a small epithelial rudiment, surrounded by mesenchymal cells. The rudiment proliferates to form a cord of cells, which continue to divide and branch into the mesenchyme. Ongoing embryonic cytomorphodifferentiation leads to the formation of duct, terminal tubule, and proacinar cells. In the newborn, both ductal and acinar cells are already present, although the glands are very small. To attain its mature size, the SMG continues to develop through the 4th week. This involves extensive proliferation and growth of the gland, with the highest mitotic index being reached at 5 days postpartum (Devi and Jacoby 1966). Thereafter, cell proliferation begins to decline, concomitant with an increased transition of cells from neonatal phenotypes to differentiated acinar and ductal cells. Two neonatal secretory cells have been identified in rat: type I cells, potential ductal cell progenitors which produce protein C, and type III cells, putative acinar cell precursors which give rise to the B1- and B2-immunoreactive proteins, products of the ZZ3 gene (Mirels and Ball 1992; Mirels et al. 1998). With progressive differentiation, there is a marked decrease in the production of the neonatal salivary proteins and an increase in levels of the adult products, such as α-amylase. Differentiated acinar and ductal cells are polarized, with their basal surface in contact with the basal lamina and the apical surface facing lumina continuous with the exterior. Moreover, the acinar and intercalated duct cells are enveloped by the myoepithelial cells, which attach to the basal lamina.

To date, little is known about the key regulators of SMG development and function. Since, in a majority of systems, execution of developmental programs requires a coordinated interplay of cell proliferation, polarization, and differentiation, temporal and spatial regulation of these events is likely to be critical to SMG biogene-

sis. During development, immature cells engage in a proliferative cycle until, in response to differentiation signal(s), they arrest in G1 and undergo differentiation (Olson and Klein 1994). Previously we showed that the first gene of the dolichol pathway, ALG7, played an important role in the dynamics of cell cycle entry and exit in G1 (Kukuruzinska and Lennon 1995, 1999; Lennon et al. 1995, 1997; Pretel et al. 1995). Conserved in evolution (Eckert et al. 1998; Huang et al. 1998; Kukuruzinska and Robbins 1987; Rajput et al. 1994; Scocca and Krag 1990; Zhu and Lehrman 1990), ALG7 encodes the dolichol-P-dependent *N*-acetylglucosamine transferase, GPT, the tunicamycin-sensitive enzyme that catalyzes the first committed step in the dolichol pathway. We also showed that GPT was a useful in vivo marker for salivary cell proliferation, because the postnatal development of the hamster SMG correlated with downregulation of ALG7 expression on the level of transcript accumulation and the activity of GPT (Fernandes et al. 1998; Mota et al. 1994).

Regulated changes in the actin cytoskeleton constitute an intricate component of tissue development. Variations in cell shape, in response to either extracellular or intracellular signals, occur through a communication of complex networks of proteins with actin filament bundles (Burridge et al. 1988). During development, actin plays a critical role in determining cell shape and movement, as well as its final function. Since changes in the salivary cell shape are vital for the acquisition of polarity and exocrine function, expression and distribution of filamentous actin is likely to reflect the extent of salivary cell differentiation.

The actin cytoskeleton is linked to the extracellular matrix by extracellular matrix receptors known as integrins, a family of heterodimeric glycoproteins each composed of an α- and a β-subunit. In response to extracellular matrix ligand engagement, integrins form dynamic clusters which, in turn, lead to the formation of focal adhesion complexes at the cytoplasmic face (Hynes 1992). One integrin receptor, β1, serves as a heterodimeric partner to a number of α-integrins. Through its association with these different α-subunits, β1 functions as a receptor for laminin, fibronectin, tenascin, and collagen type IV. On a mechanistic level, β1 links the extracellular matrix outside the cell with the actin cytoskeleton inside the cell via the network of focal contact-associated proteins (Sastry and Horitz 1993; Watt and Hertle 1994). Thus, its expression and distribution is likely to be interdependent with the organization of the actin cytoskeleton. Since β1 has been shown to function in epithelial cell migration and differentiation, this integrin is likely to participate in various aspects of SMG development.

In order to assess how cell proliferation is coordinated with cytoarchitectural and adhesive changes during SMG development, we examined the localization of GPT, filamentous actin, and β1 integrin during several distinct stages of the hamster SMG postnatal cytomorphodifferentiation using an immunohistochemical approach coupled with confocal imaging. We report that early SMG development entails extensive cell proliferation, with large numbers of cells undergoing cytoskeletal reorganization and displaying poorly defined β1 integrin along the basal lamina. With progressive development, proliferation decreases significantly, coincident with regionalized changes in cytoarchitectural and adherence characteristics of salivary cells. Differentiated SMG consists primarily of unproliferating, polarized cells with cortically organized actin and basally distributed β1 integrin. Our results indicate that SMG development entails temporal and spatial coordination of proliferative, cytoskeletal, and adhesive processes.

Materials and methods

Reagents

Primary antibodies for the neonatal salivary protein markers were rabbit antibodies against rat ZZ3 (Mirels and Ball 1992) and protein C (Ball et al. 1988), and they were provided by Lily Mirels, University of California, Berkeley. The monoclonal mouse antibody against hamster β1 integrin (clone 7E2) was purchased from Pharmingen (San Diego, Calif.). Monoclonal mouse antibodies against human β-actin and polyclonal rat antibodies against human salivary α-amylase were purchased from Sigma (St. Louis, Mo.). Polyclonal rabbit antibodies against the ALG7 protein, GPT, were either provided by Inder K. Vijay, University of Maryland, or they were commercially prepared (Babco, Berkeley, Calif.). In both cases, anti-GPT antisera were raised against a synthetic peptide sequence to the 11 C-terminal amino acids of hamster GPT. Phalloidin, conjugated with FITC or rhodamine (Molecular Probes, Eugene, Ore.), was used for the visualization of F-actin, as indicated. Secondary antibodies consisted of goat anti-rabbit IgG(Fc) or sheep anti-mouse IgG(Fc), derivatized with FITC (Molecular Probes) or horseradish peroxidase (HPR; Amersham Life Science, Arlington Heights, Ill.). Timed-pregnant hamsters were purchased from Charles River Labs (Boston, Mass.) and housed at the Boston University Medical Center (BUMC) Laboratory Animal Science facility.

Tissue preparation

At 2, 5, and 14 days after birth, as well as adult, animals were killed by exposure to CO_2 followed by cervical dislocation, as per BUMC institutional guidelines, and SMGs were isolated as described previously (Mota et al. 1994). For immunoblot analysis, glands were immediately placed on dry ice and stored frozen at −80º C until required. For confocal imaging dissected glands were fixed for 30 min in 4% paraformaldehyde in PBS (pH 7.4), and then stored in PBS at 4º C prior to staining.

Immunofluorescence

The staining procedures for confocal analyses were as follows. The glands were tweezed apart into 1-mm fragments, permeabilized with 3% Triton X-100, and washed 3 times in PBS for 15 min at room temperature. F-actin was stained with FITC-phalloidin for 30 min in the dark, and then samples were washed 3 times in PBS for 15 min at room temperature. For immunostaining, the samples were blocked with goat antiserum to prevent non-specific binding, rinsed with PBS, and stained with primary antibodies for 2 h at room temperature. The antibody to hamster β1 integrin was used at a dilution of 1:500, while antibody to hamster GPT was used at 1:5000 dilution. The excess primary antibody was removed by three 15-min washes in PBS, and the tissues were incubated with

FITC-tagged goat anti-rabbit or sheep anti-mouse IgGs as secondary antibodies (1:500) at room temperature. The excess secondary antibody was removed by four 15-min washes in PBS at room temperature. In some cases, in order to better visualize the architecture of the tissue, SMGs were simultaneously double stained with phalloidin tagged with rhodamine and with primary antibodies specific for the protein of interest followed by FITC-conjugated secondary antibodies. Samples were mounted in antifade medium on slides with nail polish spacers, coverslipped, and viewed on a confocal microscope.

Confocal imaging

Immunohistochemical staining was analyzed with a Leitz (Leica USA, Deerfield, Ill) confocal laser scanning microscope (with argon laser). For single staining of F-actin with FITC-tagged phalloidin, a series of optical sections of day 5 SMGs were taken at 0.25-µm intervals at 500× magnification. Typically, a conglomeration of eight images, at 200× magnification, was used per image printout for each developmental time course. In cases where double staining was used, confocal images reflect scans through a plane of representative optical sections 1 µm thick, at 200× magnification.

Western blot analysis

Postnatal stage-specific SMGs were homogenized on ice in RIPA buffer (50 mM TRIS, pH 6.8, 5 mM EDTA, 150 mM NaCl, 1% NP-40, 0.1% sodium deoxycholate, 0.1% SDS) containing 500 µg/ml leupeptin, 50 mM PMSF, 10 mM benzamidine, 5 mg/ml aprotinin, and 2.5 mg/ml soybean trypsin inhibitor. Following homogenization, samples were incubated in RIPA buffer supplemented with protease inhibitors for 30 min at 0º C. Chinese hamster ovary (CHO) cells (CHO 1–15000) were purchased from ATCC (Rockville, Md.), grown in F-12 media supplemented with 10% NBS, 100 U/ml penicillin, 100 µg/ml streptomycin, and 250 ng/ml of amphotericin B (Life Technologies, Gaithersburg, Md.), and harvested at 30% and 100% confluency. Cells were pelleted, washed with PBS, resuspended in RIPA buffer containing protease inhibitors (see above), and homogenized on ice. Protein concentrations were determined using a BCA protein assay (Pierce, Rockford, Ill.). The homogenates were then diluted with an equal volume of 2× Laemmli buffer, boiled for 5 min, and centrifuged, and samples (45–100 µg, as indicated) were subjected to electrophoresis using precast 8% (protein C, ZZ3, and α-amylase) or 12% (β-actin, β1 integrin, and GPT) TRIS-glycine gels against Multimark standards (Novex, San Diego, Calif.) under reducing conditions. Gel contents were transferred to nitrocellulose membranes using a Novex XCell II Blot; membranes were air dried overnight, and then blocked in PBS-T, 10% non-fat dry milk for 1 h at room temperature. Blots were incubated consecutively with primary antibodies, either anti-rat protein C (1:500), anti-rat ZZ3 (1:5000), anti-hamster GPT (1:5000), anti-human salivary α-amylase (1:2000), anti-human β-actin (1:500), anti-hamster β1 integrin (1:2000), or the corresponding preimmune sera, and secondary (HRP-conjugated anti-rabbit or anti-mouse IgG) antibodies (1:3000), and developed with ECL detection reagents, as per the manufacturer's instructions (Amersham). For peptide competition study, anti-hamster GPT (1:5000) was preincubated with antigenic peptide (10 µg/ml) at 37º C for 1 h prior to incubation with blot. Images were captured on Reflection autoradiography film (Dupont/NEN, Bosten, Mass.), and signal intensities were quantified using Kodak Digital Science 1D Software (Eastman Kodak, Rochester, N.Y.), version 1.0.2. Amounts of samples and the exposure times were chosen to assure linearity of the signal. Typically, immunoblots were performed several times with SEM indicated.

Results

Immediately after birth, the SMG begins to undergo extensive proliferation, with the mitotic index reaching the highest value within 5 days postpartum (Devi and Jacoby 1966). Thereafter, this high proliferative activity begins to decline, concomitant with an increased transition of cells from neonatal phenotypes to differentiated acinar and ductal cells. In order to assess expression and distribution of GPT and other developmentally relevant proteins during SMG postnatal development, the following stages of cytomorphodifferentiation were examined: 2 days postpartum, when cells begin to proliferate extensively; 5 days postpartum, reflecting a high mitotic index and the transition from undifferentiated cells of the ter-

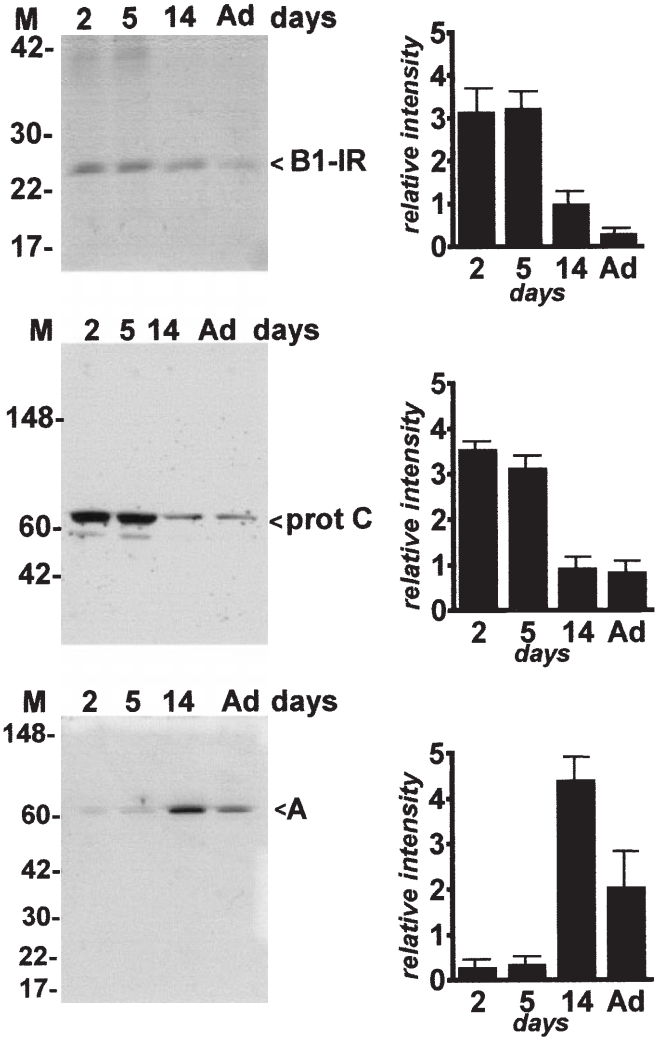

Fig. 1 Immunodetection of B1-immunoreactive proteins (*B1-IR*), protein C (*prot C*) and α-amylase (*A*) in the postnatally developing hamster submandibular gland (SMG). Tissue homogenates (100 µg for B1-immunoreactive proteins and 45 µg for protein C and α-amylase) from indicated developmental time points were analyzed by western blotting. The results are an average of four independent determinations, with the standard error of the mean (SEM) shown. *M* Multimark molecular weight standards (Novex), *Ad* adult

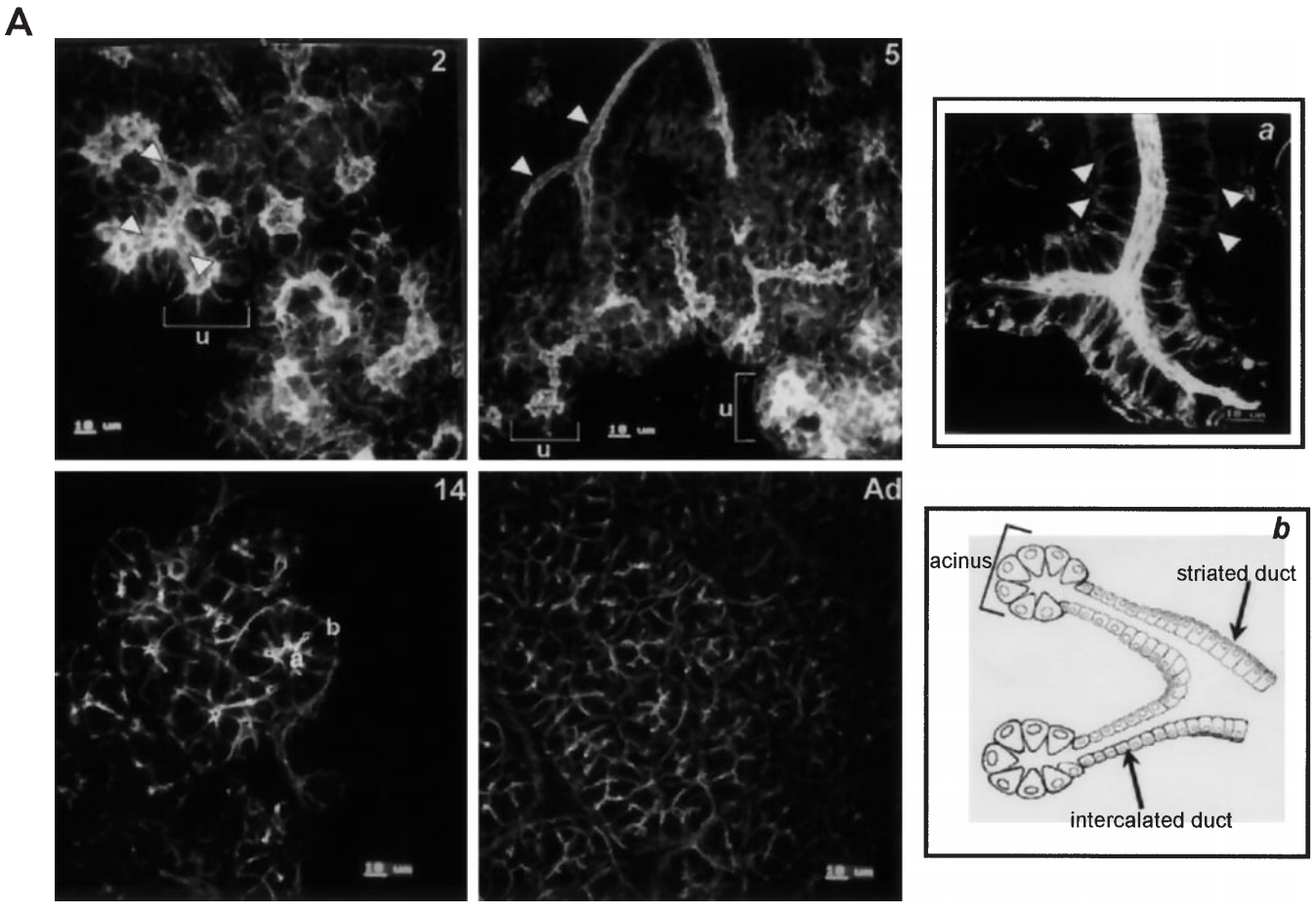

Fig. 2A, a, B, b Characterization of actin expression in the postnatally developing hamster SMG. **A** Confocal micrographs of postnatal stage-specific hamster SMGs stained with FITC-phalloidin. Each image print-out represents a conglomeration of eight images, 1 μ thick with 2 μ spacings. In 2-day-old SMGs (*2*), short, intercalated ducts display intense, apical staining (*arrows*). Terminal secretory units (*u*) are indicated. Long and branched ducts are detectable (*arrows*) in 5-day-old SMGs (*5*), with apical regions highly stained. The 14-day-old SMG (*14*) shows cortical actin staining, most intense in the apical portions of ductal and myoepithelial cells. *a* Apical, *b* basal. Adult SMGs (*Ad*) display staining of cortical actin and myoepithelial cells. **a** Close-up of day 14 SMG showing basal striations of striated duct cells (*arrows*). **b** Schematic representation of the adult SMG, with acini, and intercalated and striated ducts indicated **B** Western blot analysis of β-actin levels during postnatal development of hamster SMG. Each developmental time point represents 100 μg of total tissue homogenate protein. The results are an average of four independent determinations; the SEM is indicated. *M* Multimark molecular weight standards (Novex) *Ad* adult

minal tubules into terminal buds; 14 days after birth, when proliferation becomes abated and many acini and ducts acquire fully differentiated, functional phenotypes; and adult, with acini completely replacing the terminal buds and ducts grown to mature size, each comprising polarized, functionally differentiated cells.

The differentiation status of the hamster SMG at the distinct postnatal stages was determined by examining the production of the neonatal secretory proteins, B1 and protein C, and differentiation-specific α-amylase (Fig. 1). Although transient production of B1 by the rat SMG type III cells has been reported (Ball et al. 1988), it was unclear whether this protein was synthesized in hamster. Antibodies raised against the rat B1 (Mirels and Ball 1992) were cross-reactive with the hamster SMG proteins, exhibiting electrophoretic mobility predicted for the rat protein of approximately 27 kDa (Fig. 1). B1-immunoreactive proteins were detected in the highest amounts at days 2 and 5 of the postnatal period, declining more than threefold at 14 days postpartum. Interestingly, this protein was also detected in tissue homoge-

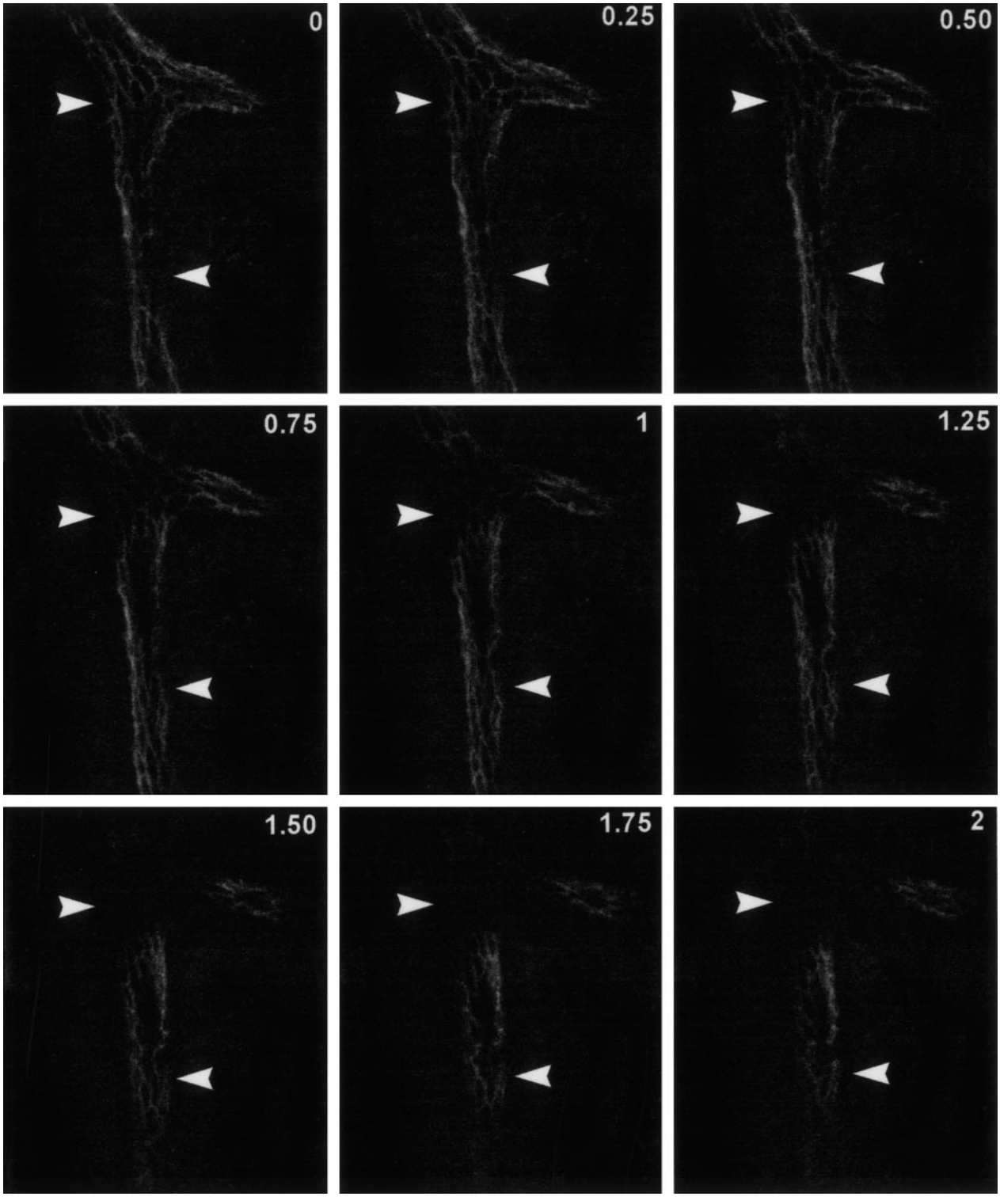

Fig. 3 Actin distribution in ductal cells of day 5 SMGs. Confocal images of day 5 SMGs stained for filamentous actin with rhodamine-conjugated phalloidin. Glands were viewed on a Leitz (Leica) confocal scanning microscope (with argon laser) at 500× magnification. Images are consecutive scans through tissue at 0.25-µm intervals, from 0 to 2 µm as indicated. *Arrows* point to F-actin, as optical sections move away from the apical regions of the cells lining the duct

nates from the adult SMGs. Also, the abundance of protein C was high in days 2–5 postpartum, reaching the lowest level in the functionally differentiated adult gland (Fig. 1). As in rat, the hamster SMG protein C migrated with the molecular weight of 89 kDa (Ball et al. 1988). In contrast, the amount of hamster SMG α-amylase increased during postnatal development from barely detectable at day 2 to a maximal value at day 14, after

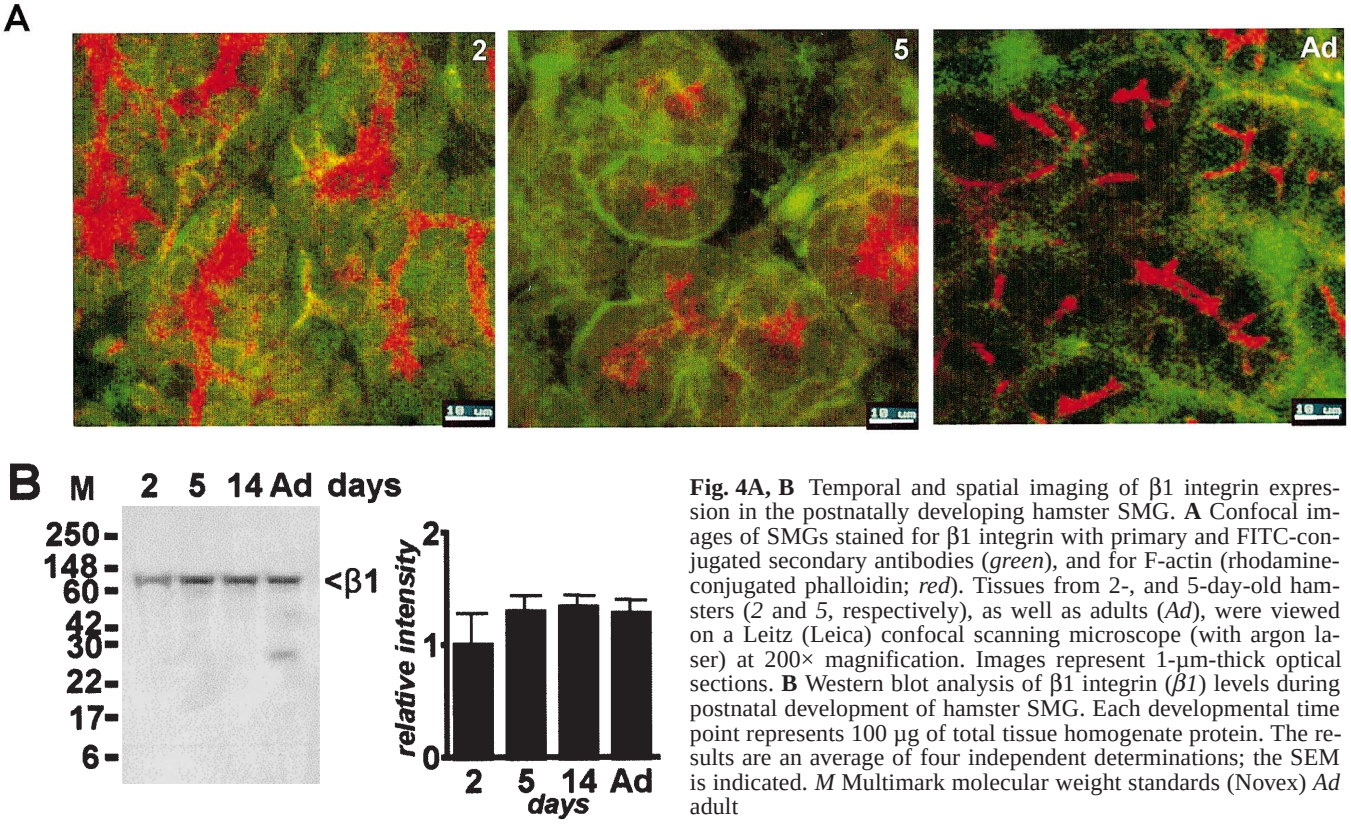

Fig. 4A, B Temporal and spatial imaging of β1 integrin expression in the postnatally developing hamster SMG. **A** Confocal images of SMGs stained for β1 integrin with primary and FITC-conjugated secondary antibodies (*green*), and for F-actin (rhodamine-conjugated phalloidin; *red*). Tissues from 2-, and 5-day-old hamsters (*2* and *5*, respectively), as well as adults (*Ad*), were viewed on a Leitz (Leica) confocal scanning microscope (with argon laser) at 200× magnification. Images represent 1-µm-thick optical sections. **B** Western blot analysis of β1 integrin (*β1*) levels during postnatal development of hamster SMG. Each developmental time point represents 100 µg of total tissue homogenate protein. The results are an average of four independent determinations; the SEM is indicated. *M* Multimark molecular weight standards (Novex) *Ad* adult

which its levels declined to approximately 60% of the day 14 value in the adult (Fig. 1). No signals were detected when preimmune sera were used instead of primary antibodies for B1-immunoreactive proteins, protein C, and α-amylase (data not shown). The decline in the α-amylase abundance in the adult tissue homogenates compared to the 14-day-old stage may reflect a dilution effect due to an increase in the relative levels of other adult SMG proteins.

Cytoarchitectural characteristics of the developing SMG in vivo were ascertained with confocal microscopy (Paddock 1994) using phalloidin to visualize F-actin localization and distribution (Fig. 2A). Phalloidin staining also provided an image of the organization of cells within the developing tissue (see schematic, Fig. 2b). In the 2-day-old glands, cortical actin delineated extensive lobulation as well as branching of ducts, although at this stage the ducts were short with highly stained luminal regions (Fig. 2 A). The staining of lobules is likely to reflect cortical actin of salivary cells and, possibly, the surrounding myoepithelial cells. The most intense F-actin staining was localized to the apical regions of cells in the terminal secretory units. This accumulation of F-actin in the terminal branches suggested that cytoarchitectural reorganization might be taking place, and that the latter might be involved in the polarization that accompanies cytodifferentiation of the immature acini and intercalated ducts. In the 5-day-old gland, the ducts were much longer compared to the 2-day-old tissue, indicating that they underwent significant growth and branching between 2 and 5 days postpartum (Fig. 2A). At 5 days, some of the terminal secretory units still displayed intense actin staining, suggesting ongoing cytodifferentiation of acini and intercalated ducts. By day 14 postpartum, many terminal secretory units reached their mature size, with intense cortical actin staining in the apical regions of cells (Fig. 2A). Characteristic of differentiated striated ducts, cells with basal striations and large nuclei, as well as strong apical actin concentration, were detected (Fig. 2a). In the adult gland, the overall phalloidin staining was much lower compared to the neonatal SMG and limited primarily to cortical actin, which remained more pronounced in the apical regions of ducts (Fig. 2A).

A noted decline in the levels of actin expression with progressive SMG differentiation has not been described before. The abundance of total actin during the postnatal development of SMG was also assessed with immunoblotting (Fig. 2B). The levels of actin expression followed the pattern observed with confocal imaging of F-actin, being high in the neonatal glands and declining sharply with differentiation (Fig. 2B). Since actin has been shown to be regulated with growth, such downregulation of actin expression with diminished proliferation is expected (Lau and Nathans 1987).

Spatial distribution of F-actin during SMG postnatal development was further investigated in tissue samples stained with rhodamine-conjugated phalloidin, optically sectioned at 0.25-µm intervals (Fig. 3). The dramatic images allow visualization of F-actin as sections move away from the apical regions of the cells lining the duct.

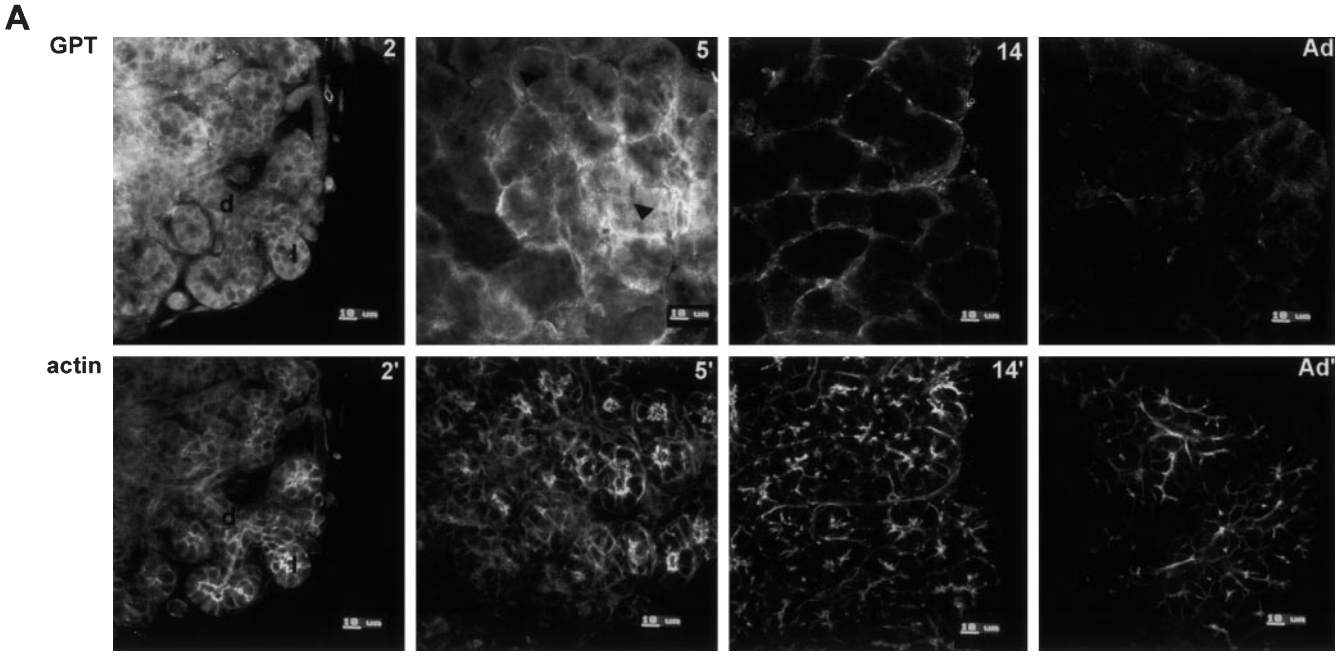

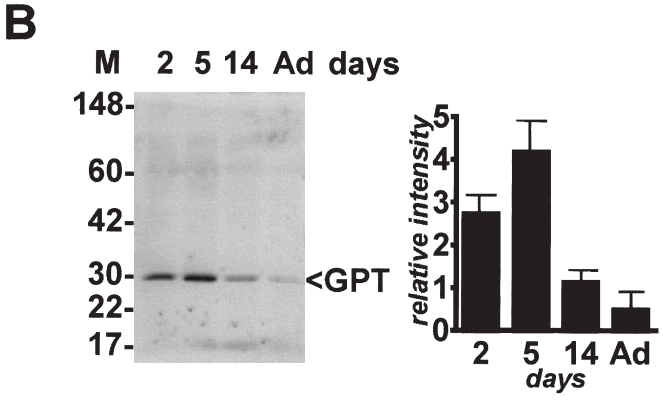

Fig. 5A, B Temporal and spatial imaging of GPT expression in the postnatally developing hamster SMG. **A** Confocal micrographs of SMGs double stained with polyclonal anti-hamster GPT (*2*, *5*, *14*, and *Ad*) and rhodamine-phalloidin (*2′*, *5′*, *14′*, and *Ad′*). The secondary antibody was goat anti-rabbit heavy and light chain IgG conjugated to FITC. Representative duct (*d*) and lumen (*l*) in a 2-day-old gland (*2* and *2′*) are indicated. Localized areas of high and low intensity staining in a 5 day-old gland (*5* and *5′*) are indicated (*arrows*). *14*, *14′* 14-day-old SMG, *Ad*, *Ad′* adult SMG. **B** Western blot analysis of GPT levels during the postnatal development of hamster SMG. Each developmental time point represents 100 µg of total tissue homogenate protein. The results are an average of four independent determinations; the SEM is indicated. *M* Multimark molecular weight standard (Novex)

The top arrow indicates that actin localizes primarily to the apical regions of duct cells. The bottom arrow is for reference as the optical sections pass through different planes of the duct.

Changes in the distribution and abundance of actin during postnatal development suggested that immature salivary glands underwent reorganization during the early stages of the postnatal period. To examine this notion further, we determined the expression and distribution of β1 integrin, a heterodimeric partner to various α integrins and member of a family of transmembrane receptors that mediate both cell-cell and cell-matrix interactions (Fig. 4). These tissues were double stained with anti-β1 integrin antibody (green) and phalloidin (red). Although in the neonate, some of the β1 integrin was already localized to the basal lamina, a significant fraction of the protein appeared dispersed over the cell membrane (Fig, 4A). The localization of β1 to the basal membrane increased from day 2 to day 5 (Fig. 4A). In the adult, β1 was limited to regions where cells interact with basal lamina (Fig. 4A). Some of the β1 integrin staining may reflect its presence in myoepithelial cells. Immunoblot analysis showed that although the distribution of β1 integrin was dramatically altered during SMG postnatal development, its levels were not significantly modulated (Fig. 4B).

The temporal and spatial expression of GPT was evaluated using double staining of developmental-stage specific SMGs with anti-GPT antisera and phalloidin (Fig. 5). The highest level of staining was detected in the neonatal, 2-, and 5-day-old glands, compared to later postnatal stages (Fig. 5A). In the 2-day-old gland, most cells, including the terminal secretory units and ducts, exhibited an evenly distributed staining. This stage of postnatal development correlates with a high mitotic activity of the gland (Devi and Jacoby 1966), reflective of active proliferation of the terminal secretory units and ducts. A direct comparison of this section stained for GPT and actin showed that both acini and ducts were labeled, while luminal regions were negative (Fig. 5A). The even distribution of GPT, an ER membrane protein, in cells of neonatal glands is likely to reflect their unpolarized nature.

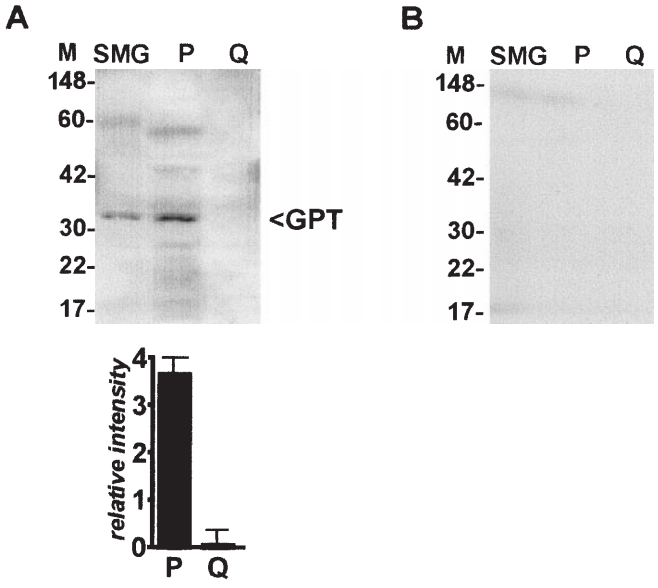

Fig. 6 Growth-dependent GPT expression in Chinese hamster ovary cells. Cell lysates (100 μg), prepared from cells grown to either 30% (*P*) or 100% (*Q*) confluency, were analyzed for GPT expression by western blotting. For comparison, homogenates (100 μg) from day 5 hamster SMGs (*SMG*) were used. The results are an average of three independent experiments; the SEM is illustrated. As a control to show specificity of the antibody, anti-hamster GPT was preincubated with an excess of antigenic peptide prior to incubation with the blot. *M* Multimark molecular weight standard (Novex)

The staining characteristics were altered in the 5-day-old glands, which displayed high GPT expression only in certain regions of the gland, becoming abated in others (Fig. 5A). It is likely that regions with abundant, evenly distributed GPT represent proliferating cells of the developing terminal secretory units. At the 14-day stage, when many cells displayed already differentiated phenotypes, the amount of GPT-specific staining declined significantly, being limited primarily to basal regions. Since in polarized salivary cells, ER is at the basal surface, the GPT staining appears to reflect the highly differentiated status of the tissue at this stage of development (Fig. 5A). In the adult gland, all GPT-specific staining was detected only along the basal lamina (Fig. 5A), although it is also possible that some of the GPT was in myoepithelial cells. No signal was detected when preimmune serum was used instead of primary antibody (data not shown). These results further support the previously reported studies which showed that tunicamycin, an inhibitor of GPT, dramatically decreased epithelial cell proliferation but not branching (Bassett and Spooner 1987). Immunoblot analysis of GPT in the postnatally developing SMG showed that the amount of GPT correlated with the proliferative activity of the gland, increasing from 2 to 5 days postpartum and then becoming progressively attenuated with diminished cell division, reaching the lowest level in the functionally differentiated adult tissue (Fig. 5B). Although the predicted molecular weight of hamsters GPT is 46 kDa, it has been reported to display aberrant mobility upon electrophoresis, 33–36 kDa, even in the presence of protease inhibitors (Scocca et al. 1995; Huang et al. 1998). The specificity of the anti-GPT antibody was confirmed in a competition study in which a 10-μg/ml antigenic peptide was incubated with the antibody (1:5000 dilution) at 37° C for 1 h prior to western blot analysis (Fig. 6). No signal was detected when preimmune serum was used instead of the primary antibody (data not shown).

Spatial and temporal analyses using confocal imaging localized GPT to unpolarized, highly proliferative regions of the gland (Fig. 5A). Moreover, immunoblot assays of GPT at the distinct developmental stages showed that its abundance correlated with a high proliferative activity of the neonatal glands (Fig. 5B). Therefore, similar to yeast (Kukuruzinska and Lennon 1994), ALG7 expression in hamster SMG was proliferation dependent, being attenuated with growth arrest and differentiation. This proliferation-dependent behavior of hamster GPT was confirmed in actively dividing versus growth-arrested CHO cells (Fig. 6). As expected, GPT from the CHO cells migrated with the same mobility, 33 kDa, as the species from the 5-day-old SMG.

Discussion

To date, little is known about genetic programs regulating mammalian salivary gland development. Similar to other developing tissues, however, they are likely to entail a coordinated interplay of proliferation, morphogenesis, and cell-substratum interactions. Indeed, confocal analyses presented here provide evidence that hamster SMG development is a complex process involving regionalized proliferation and differentiation. Judging by the levels of expression and distribution of GPT, actin, β1 integrin, and neonatal and differentiation-specific proteins, the early stages of SMG postnatal development entail primarily cell proliferation, with differentiation becoming predominant by day 14 and continuing into the adult state. Our studies also show that variations in the relationships among GPT, actin, and β1 integrin expression determine the differentiation state of salivary cells within the developing tissue. Because salivary cell proliferation and differentiation appear to be opposing processes, SMG development resembles the paradigm of other developing systems, where the markers of differentiation are not expressed until cells exit the cell cycle (Olson and Klein 1994).

The observation regarding the high proliferative activity in the neonatal hamster SMG was reported previously (Devi and Jacobi 1996). The confocal imaging data and immunoblotting assays show that the abundance of GPT correlates with cell proliferation, cytoskeletal rearrangement, and redistribution of cell surface receptors. At day 2 postpartum, a majority of cells displays high levels of GPT expression. Specifically, in the immature cells of the terminal secretory units, GPT is evenly distributed. Moreover, the temporal expression of GPT parallels that of B1-immunoreactive proteins and protein C, the previously reported

markers for the neonatal proacinar (type III) and productal (type I) cells in the rat SMG, respectively (Ball et al. 1988; Denny et al. 1997; Mirels and Ball 1992). Based on the temporal nature of the inverse relationship between neonatal and differentiation-specific proteins, these data indicate that at days 2 and 5, the majority of cells are immature and that they become differentiated by day 14.

Imaging of actin alone clearly delineates the rounded morphology of immature salivary cells. Because these cells appear unpolarized, and because ALG7 belongs to a class of early growth response genes (Kukuruzinska and Lennon 1994), most of the cells exhibiting high levels of GPT are likely to be engaged in the cell cycle. The proliferation-dependent nature of GPT is also supported by our results with actively dividing and quiescent CHO cells (Fig. 6). Furthermore, recent studies suggest that dolichol phosphate, one of the substrates of GPT, is a regulator of cell growth by affecting *N*-glycosylation of the IGF-1 receptor (Dricu et al. 1997). Taken together, these results align high levels of GPT expression with proliferation of immature salivary cells, and confirm our previously reported RNA blotting and GPT activity studies (Mota et al. 1994). Similar downregulation of GPT during development has been reported for the murine mammary gland (Ma et al. 1996).

The dispersed distribution of β1 integrin in the neonatal glands, when the mitotic index at its highest level, indicates that stable adhesive interactions are not established during active tissue proliferation. Since β1 functions in cell-substratum and cell-cell adhesions, our data suggest that in the neonatal glands stable adhesive complexes are not formed most likely to allow for proliferation to proceed.

The proliferation pattern of the developing SMG is altered by 5 days postpartum, when some regions of the gland continue to express high levels of GPT, but others already show its attenuated abundance (Fig. 5A). Because the actual growth of the gland increases from day 2 to day 5, the overall level of GPT in gland homogenates may in fact be higher at day 5 compared to day 2, as indicated by immunoblot analysis (Fig. 5B). The cells with diminished GPT expression display polarized morphology and extensive apical actin distribution, suggesting that they had undergone reorganizational changes in the actin cytoskeleton. Moreover, at this stage, β1 integrin becomes more clearly localized along the basal lamina, suggesting that stable adhesive complexes are being established. These variations in levels and distribution of GPT, actin, and β1 integrin indicate that at 5 days after birth, SMG is engaged in the process of regionalized proliferation and differentiation. The latter becomes more apparent at an advanced stage of postnatal development, day 14, when fully differentiated cells and glandular structures are prominent.

The abundance of GPT is attenuated significantly in polarized cells, being limited to the basal regions, typical of the ER localization in differentiated salivary cells. Similar to GPT, levels of actin are also much lower in differentiated salivary cells, detected primarily in the cortical regions. Although the extent of β1 integrin expression is not greatly altered with progressive development, upon differentiation it becomes localized to adhesive structures along the basal lamina. This may reflect that changes in β1 integrin heterodimer affinity are involved in the regulation of SMG morphogenesis.

The studies reported here indicate that SMG development entails temporal and spatial coordination among cell proliferation, cytoarchitectural organization, and the establishment of stable cell-substratum interactions. Each of the protein markers examined here, GPT, F-actin, and β1 integrin, is itself functionally important and, most likely, regulatory. Moreover, it is possible that these and other proteins affecting proliferation, polarization, and adhesion interact with each other, either directly or indirectly, making the above processes interdependent. For instance, GPT is likely to affect various aspects of SMG development by regulating the *N*-glycosylation capacity of proliferating and differentiating cells (Rademaker et al. 1988). Recent studies show that polarized growth of yeast cells is dependent on *N*-glycosylation (Mondesert et al. 1997). In epithelial cells, *N*-glycans have been suggested to function in polarized secretion, most likely by serving as sorting signals (Fiedler and Simons 1995). Indeed, inhibition of GPT activity with tunicamycin interferes with the apical secretion of the major glycoprotein, clusterin (gp80) in Madin-Darby canine kidney cells (Urban et al. 1987). Hence, changes in the levels of GPT reported here may themselves be necessary for the events directing salivary cell proliferation, polarization, and differentiation at distinct developmental stages. Likewise, alterations in the organization and distribution of F-actin and β1 integrin may affect the expression of GPT and each other. Further studies, based on perturbing these proteins' expression and observing the phenotypic consequences, are needed to assess their functional significance in salivary gland development.

Acknowledgements We would like to thank Drs. Inder Vijay, Lily Mirels, and William Ball for providing us with relevant antibodies and for helpful discussions. This research was supported by grants RO1DE-10183, RO1DE-10183-S1, and KO4DE-00362 from the National Institute of Dental Research, National Institutes of Health, U.S. Public Health Service.

References

Ball WD, Hand AR, Johnson AO (1988) Secretory proteins as markers for cellular phenotypes in rat salivary glands. Dev Biol 125:265–279

Bassett KE, Spooner BS (1987) An autoradiographic analysis of *N*-linked glycoconjugates in embryonic salivary gland morphogenesis. J Exp Zool 242:317–324

Burridge K, Fath K, Kelly T, Nuckolls G, Turner C (1988) Focal adhesions: transmembrane junctions between the extracellular matrix and the cytoskeleton. Annu Rev Cell Biol 4:487–525

Chaudhry AP, Cutler LS, Schmutz JA Jr, Yamane GM, Sunderraj M, Pierri LK (1985) Development of the hamster submandibular gland. I. The acinar-intercalated duct complex. J Submicrosc Cytol 17:555–567

Denny PC, Ball WD, Redman RS (1997) Salivary glands: a paradigm for diversity of gland development. Crit Rev Oral Biol Med 8:51–75

Devi NS, Jacoby F (1966) The submaxillary gland of the golden hamster and its postnatal development. J Anat 100:269–285

Dricu A, Wang M, Hjertman M, Malec M, Blegen H, Wejde J, Carlberg M, Larsson O (1997) Mevalonate-regulated mechanisms in cell growth control: role of dolichyl phosphate in expression of the insulin-like growth factor-1 receptor (IGF-1R) in comparison to Ras prenylation and expression of c-myc. Glycobiology 7:625–633

Eckert V, Blank M, Mazhari-Tabrizi R, Mumberg D, Funk M, Schwarz RT (1998) Cloning and functional expression of the human GlcNAc-1-P transferase, the enzyme for the committed step of the dolichol cycle, by heterologous complementation in *Saccharomyces cerevisiae*. Glycobiology 8:77–85

Fernandes R, Fox M, Cotanche DA, Lennon K, Kukuruzinska MA (1998) Confocal imaging of gene expression during hamster salivary gland biogenesis. Ann NY Acad Sci 842:212–216

Fiedler K, Simons K (1995) The role of *N*-glycans in the secretory pathway. Cell 81:309–312

Huang GT-J, Lennon K, Kukuruzinska MA (1998) Characterization of multiple transcripts of the hamster dolichol-P-dependent *N*-acetylglucosamine-1-*P* transferase suggests functionally complex expression. Mol Cell Biochem 181:97–106

Hynes RO (1992) Integrins: versatility, modulation, and signaling in cell adhesion. Cell 69:11–25

Kukuruzinska MA, Lennon K (1994) Growth-related coordinate regulation of the early *N*-glycosylation genes in yeast. Glycobiology 4:437–443

Kukuruzinska MA, Lennon K (1995) Diminished activity of the first *N*-glycosylation enzyme, dolichol-P-dependent *N*-acetylglucosamine-1-P transferase (GPT), gives rise to mutant phenotypes in yeast. Biochim Biophys Acta 1247:51–59

Kukuruzinska MA, Lennon-Hopkins K (1999) ALG gene expression and and cell cycle progression. Biochim Biophys Acta 1426: in press

Kukuruzinska MA, Robbins PW (1987) Protein *N*-glycosylation in yeast: transcript heterogeneity of the ALG7 gene. Proc Natl Acad Sci USA 84:2145–2149

Lau LF, Nathans D (1987) Expression of growth-related immediate early genes in BALB/c 3T3 cells: coordinate regulation with *c-fos* or *c-myc*. Proc Natl Acad Sci USA 84:1182–1186

Lennon K, Pretel R, Kesselheim J, Heesen S te, Kukuruzinska MA (1995) Proliferation-dependent differential regulation of the dolichol pathway genes in *Saccharomyces cerevisiae*. Glycobiology 5:633–642

Lennon K, Bird A, Kukuruzinska MA (1997) Deregulation of the first *N*-glycosylation gene, ALG7, perturbs the expression of G_1 cyclins and cell cycles arrest in *Saccharomyces cerevisiae*. Biochem Biophys Res Commun 273:562–565

Ma J, Saito H, Oka T, Vijay IK (1996) Negative regulatory element involved in the hormonal regulation of GlcNAc-1-P transferase gene in mouse mammary gland. J Biol Chem 271:11197–11203

Mirels L, Ball WD (1992) Neonatal rat submandibular gland protein SMG-A and parotid secretory protein are alternatively regulated members of a salivary protein multigene family. J Biol Chem 267:2679–2687

Mirels L, Miranda AJ, Ball WD (1998) Characterization of the rat salivary gland B1-immunoreactive proteins. Biochem J 330: 437–444

Mondesert G, Clarke DJ, Reed SI (1997) Identification of genes controlling growth polarity in the budding yeast *Saccharomyces cerevisiae*: a possible role of *N*-glycosylation and involvement of the exocyst complex. Genetics 147:421–434

Mota OM, Huang GT, Kukuruzinska MA (1994) Developmental regulation and tissue-specific expression of hamster dolichol-P-dependent *N*-acetylglucosamine-1-P transferase (GPT). Biochem Biophys Res Commun 204:284–291

Olson EN, Klein WH (1994) bHLH factors in muscle development: dead lines and commitments, what to leave in and what to leave out. Genes Dev 8:1–8

Paddock SW (1994) To boldly glow ... applications of laser scanning confocal microscopy in developmental biology. Bioessays 16:357–365

Pretel R, Lennon K, Bird A, Kukuruzinska MA (1995) Expression of the first *N*-glycosylation gene in the dolichol pathway, ALG7, is regulated at two major control points in the G_1 phase of the *Saccharomyces cerevisiae* cell cycle. Exp Cell Res 219:477–486

Rademacher TW, Parekh RB, Dwek RA (1988) Glycobiology. Ann Rev Biochem 57:785–838

Rajput B, Muniappa N, Vijay IK (1994) Developmental and hormonal regulation of UDP-GlcNAc:dolichol-phosphate *N*-acetylglucosaminephosphotransferase. Molecular cloning of the cDNA, generation of anti-peptide antibodies, and chromosomal location. Biochem J 285:985–992

Sastry SK, Horwitz AF (1993) Integrin cytoplasmic domains: mediators of cytoskeletal linkages and extra- and intra-cellular initiated transmembrane signaling. Curr Opin Cell Biol 5:819–831

Scocca JR, Krag S (1990) Sequence of a cDNA that specifies the uridine diphosphate *N*-acetyl-D-glucosamine:dolichol phosphate *N*-acetylglucosamine-1-phosphate transferase from Chinese hamster ovary cells. J Biol Chem 265:20621–20626

Scocca JR, Zou J, Krag S (1995) Genomic organization and expression of hamster UDP-*N*-acetylglucosamine:dolichyl phosphate *N*-acetylglucosaminyl phosphoryl transferase. Glycobiology 5:129–136

Urban J, Parczyk K, Leutz A, Kayne M, Kondor-Koch C (1987) Constitutive apical secretion of an 80-kD sulfated glycoprotein complex in the polarized epithelial Madin-Darby canine kidney cell line. J Cell Biol 105:2735–2743

Warr FM, Hertle MD (1994) Keratinocyte integrins. In: Leigh IM, Lane EB, Watt FM (eds) The keratinocyte handbook. Cambridge University Press, Cambridge, pp 153–164

Zhu XY, Lehrman MA (1990) Cloning, sequence and expression of a cDNA encoding hamster UDP-GlcNAc:dolichol phosphate *N*-acetylglucosamine-1-phosphate transferase. J Biol Chem 265:14250–14255